Materials Chemistry and Physics 214 (2018) 180–184

Contents lists available at ScienceDirect

Materials Chemistry and Physics

journal homepage: www.elsevier.com/locate/matchemphys

Investigation of defects dependence of local piezoelectric response on Fe, La-modified (Pb,Sr)TiO_3 thin films: A piezoresponse force microscopy study

W.B. Bastos [a], E. Longo [a], A.J. Chiquito [b], D.S.L. Pontes [c], F.M. Pontes [c, *]

[a] LIEC – Department of Chemistry, Universidade Federal de São Carlos, Via Washington Luiz, Km 235, P.O. Box 676, 13565-905, São Carlos, São Paulo, Brazil
[b] NanO LaB – Department of Physics, Universidade Federal de São Carlos, Via Washington Luiz, Km 235, P.O. Box 676, 13565-905, São Carlos, São Paulo, Brazil
[c] Department of Chemistry, Universidade Estadual Paulista - Unesp, P.O. Box 473, 17033-360, Bauru, São Paulo, Brazil

HIGHLIGHTS

- The Fe, La co-doping (Pb,Sr)TiO_3 films are fabricated by sol-gel like method.
- The defect dipoles can be reorient under an PFM tip-bias-induced electric field.
- The Fe, La co-doping (Pb,Sr)TiO_3 films behaved like ferroelectric at the nanoscale.

GRAPHICAL ABSTRACT

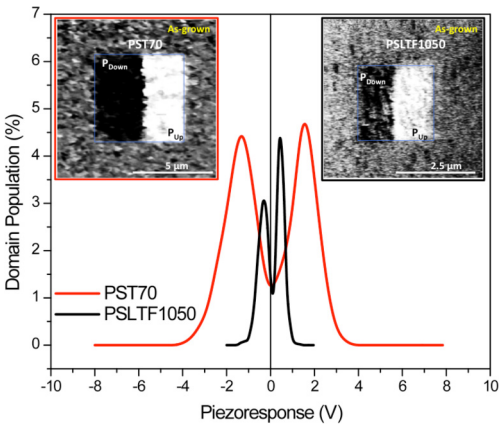

ARTICLE INFO

Article history:
Available online 24 April 2018

Keywords:
Point defects
Thin films
Piezoresponse force microscopy
Piezoelectric behavior

ABSTRACT

In this study, undoped-(Pb,Sr)TiO_3 and Fe^{3+}, La^{3+} co-doped (Pb,Sr)TiO_3 thin films were investigated at the nanoscale level by piezoresponse force microscopy (PFM), in order to evaluate the impact of doping-induced damages on the ferroelectric and piezoelectric properties. Detailed investigations with nanoscale resolution have revealed occurrence of abnormal domains in writing pattern under forward and reverse bias for (Pb,Sr,La)(Ti,Fe)O_3 thin films. Further piezoresponse hysteresis loop measurements show that fully switchable loops were observed under high voltage mediated by defect dipoles and by "ferroelectric-like" polar defects clusters. They have been discussed taking into account charged defect formation with both local changes in the dipole moment and local symmetry breaking effects. In addition, the domain writing and its retention behavior of the undoped-PST and (Pb,Sr,La)(Ti,Fe)O_3 thin films were investigated. Undoped-PST films exhibited better stability for both positive and negative domains for a relatively long time in comparison to that observed for (Pb,Sr,La)(Ti,Fe)O_3 films.

* Corresponding author.
E-mail address: fenelon@fc.unesp.br (F.M. Pontes).

https://doi.org/10.1016/j.matchemphys.2018.04.062
0254-0584/

1. Introduction

Ferroelectric materials continue to attract much attention due innumerable unique applications, for example: memory devices, infrared sensors, cell solar, energy harvesting devices, thermal imaging devices, piezo-sensors, and many more [1–5]. In particular it has been shown that doped $PbTiO_3$ oxides have been intensively studied and the results point to remarkably different electronic structure and physical properties when Pb is replaced by Ca, Sr, Ba, La and Ti by Zr, Fe, Co, Cu, Ni, Mn, Al [6–12]. Actually, $Pb_{1-x}Sr_xTiO_3$ (PST) compounds have emerged as a promising perovskite-family of functional materials [13–16]. For example, Guo et al., have reported a novel ferroelectric/gyromagnetic ferrite layered composite thin film using as ferroelectric layer $Pb_{0.4}Sr_{0.6}TiO_3$ (PST) thin films [14]. Negi et al., have prepared $NiFe_2O_4$/(Pb, Sr)TiO_3 (NFO/PST) bilayer thin films by the chemical solution method and investigated their multiferroic, magnetoelectric and magneto-impedance properties [17]. In addition, the most common application is in nonvolatility memory devices, in which is used the ability of ferroelectric thin films to maintain their polarization state in the absence of an external field even after electric writing process. However, the polarization level of ferroelectric thin films at nano or macroscopic scale is directly affected by strain/stress, presence of different defect types (extrinsic, intrinsic, charged and neutral), chemical substitution, thickness, and grain sizes (domain size) [18–21]. Several papers have focused on defects or impurities playing a dominant role in determining the ferroelectric and piezoelectric behavior at nanoscale level. Also, it is well established that point defects such as oxygen vacancies, cation vacancies and complex dipole defects can enhance, reduce or give rise to polarization behavior [22–25]. Recently, Klyukin and Alexandrov have reported on the role of intrinsic defects and defect clusters in nonferroelectric oxide, e.g., $SrTiO_3$ using density functional theory based calculations under the Berry phase approach [26]. The results show that intrinsic point defects contribute to the arising of ferroelectric polarization in $SrTiO_3$. Dutta et al. have reported this nanoscale phenomenon in $BaZrO_3$ thin films with cubic crystal structure and attributed it to polarization switching due to the point defects [27]. Recent reports by Lee et al. have shown that the defect engineering is a powerful approach for controlling local polarization switching using piezoresponse force microscopy (PFM) in $BiFeO_3$ thin film [28]. In addition, Feigl et al., have shown by PFM data that the switching in epitaxial $Pb_{0.60}Sr_{0.40}TiO_3$ ferroelectric thin films resulted in the creation of a secondary domain accompanied by a charged domain wall [29].

In this study we carried out a systematic investigation on ferroelectric and piezoelectric response at the nanoscale by means of piezoresponse force microscopy in La^{3+} (donor-like) and Fe^{3+} (acceptor-like) co-doped-(Pb,Sr)TiO_3 thin films.

2. Experiment procedure

Ferroelectric undoped-$(Pb_{0.70}Sr_{0.30})TiO_3$ (referred here as PST70) and $(Pb_{0.70}Sr_{0.20}La_{0.10})(Ti_{0.50}Fe_{0.50})O_3$ (referred here as PSLTF1050) thin films were deposited on Pt/Ti/SiO_2/Si(100) commercial substrate by chemical deposition solution method. Details of the preparation method can be found in the literature [30,31]. The precursor solution was spun on the substrate at 1000 rpm for 10 s and 5000 rpm for 30 s, using a spin coater (KW-4B, Chemat Technology) via a syringe filter to avoid particulate contaminations. After spin coating, the films were preheated to 200 °C for 10 min on a hot plate to remove residual water. Then, the films were annealed using a stepwise/successive growth and crystallization engineered method at 400 °C/4 h and 700 °C/2 h in ambient air to remove residual organic components at a heating rate of 5 °C/min, respectively. The film thickness was adjusted by repeating the deposition and the pyrolysis/growth/crystallization cycle.

Phase identification of thin films were investigated by a Rigaku D/Max 2400 X-ray diffractometer with Cu-Kα radiation. The thickness of the thin films was measured using a field-emission scanning electron microscope (FE-SEM, FEG-VP Zeiss Supra 35) with a secondary electron lens detector on a freshly fractured film/substrate cross-section. The cross-section micrographs shown that the thickness of PST70 and PSLTF1050 thin films is 220 and 200 nm, respectively. The topography, polarization pattern of ferroelectric domain structures, and local hysteresis loops were investigated at the nanoscale level on ferroelectric thin films using a commercial AFM (MultiMode Nanoscope V, Bruker) modified to be used also as a PFM. The probe used in piezoresponse measurements was the PPP-NCHR (Nanosensors). This tip is made of a highly doped silicon to dissipate static charge and has an Aluminum coating. The spring constant is 46 N/m. The system was equipped with a lock-in amplifier (SR850, Stanford) and a function generator (33220A, Agilent). During the PFM measurements, the conductive probe was electrically grounded and an external voltage was applied to the bottom Pt electrode operated with a driving amplitude of 1 V (RMS). In order to investigate the localized polarization retention behavior after electric writing process, lithography model in piezoresponse force microscopy was carried out on PST70 and PSLTF1050 thin films, i.e., a DC bias was applied to the conducting PFM-tip probeand the tip was grounded while scanning the desired area. Local poling "writing" was achieved on a square-shaped region 2 μm × 2 μm (PSLTF1050), and 5 μm × 5 μm (PST70) by alternately applying a DC voltage of −15 V (black contrast) and +15 V (bright contrast) to the conductive PFM-tip, corresponding to downward and upward polarization stable states, respectively. Then PFM images were recorded to observe the electric writing retention behavior as a function of time. All scans were performed under identical condition, with an AC field of 1V peak-to-peak applied to the tip. Piezoresponse images were carefully aligned according to the features in the topography images.

3. Results and discussion

The XRD patterns of PST70 and PSLTF1050 thin films annealed at 700 °C on Si/SiO_2/Ti/Pt substrate are given in Fig. 1(a). All thin films showed perovskite phases but presenting a polycrystalline nature. In addition, the PST70 thin films clearly revealed splitting of (001)/(100), (101)/(110), and (002)/(200) diffraction peaks, suggesting a tetragonal structure phase, as shown in Fig. 1(a). Nevertheless, a lower tetragonality character of the unit cell (leading to structural tetragonal to cubic phase transition at room temperature) was observed in Fe, La co-doped PSLTF1050 films (Fig. 1 (a)). Additionally, Raman spectroscopy was carried out to provide additional information on the structure, since this method is very sensitive to variations of local bonding, short- and medium-length range

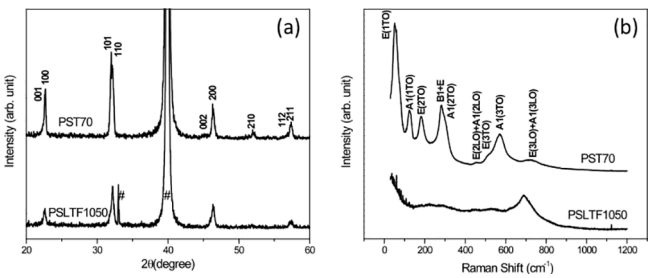

Fig. 1. (a) XRD patterns and (b) Raman spectra of PST70 and PSLTF1050 thin films annealed at 700 °C, respectively.

symmetry breaking. Raman spectra of the PST70 and PSLTF1050 thin films are shown in Fig. 1(b). The spectrum of the PST70 thin films shows the typical signature of a tetragonal perovskite phase, which is also in good agreement with the prototypical ferroelectric $PbTiO_3$ [32]. In contrast, La and Fe substitution at A- and B-sites, respectively, leads to diffuse Raman spectra in PSLTF1050 thin films. These findings clearly supports a tetragonal to pseudocubic phase transition. In addition, a careful analysis of the spectra shows that an intensity weakening and broadbands from 200 to 600 cm^{-1} and also a pronounced peak at 690 cm^{-1}. The origin of these Raman-active modes is related to short- and long-range extrinsic disorder, where atoms are shifted from their perfect symmetry positions, due to point defects, complex dipoles defects and nanoscale strain/stress.

In PSLTF1050 thin films different defects type could exist when Fe^{3+} (acceptor-like) and La^{3+}(donor-like) doping are introduced in the PST70 lattice. In this situation, the overall charge neutrality should be maintained by $Fe^{3+}$and La^{3+} doping on the Ti-sites and Sr-sites, respectively. In this scenario different and plausible compensation mechanisms should be considered for PSLTF1050 thin films. Using Kröger-Vink notation, the charge compensation equations can be represented by

$$2Fe_{Ti}^{x} \leftrightarrow 2Fe_{Ti}^{\prime} + V_{O}^{\cdot\cdot} \quad (1)$$

$$Sr_{Sr} \rightarrow La_{Sr}^{\cdot} + e^{\prime} \quad (2)$$

$$4Sr_{Sr} + Ti_{Ti} \rightarrow 4La_{Sr}^{\cdot} + V_{Ti}^{\prime\prime} \quad (3)$$

$$2Fe_{Ti}^{x} \leftrightarrow 2Fe_{Ti}^{\prime} + V_{O}^{\cdot\cdot} \quad (4)$$

$$2La_{Sr}^{x} \rightarrow 2La_{Sr}^{\cdot} + V_{Sr}^{\prime\prime} \quad (5)$$

Furthermore, the presence of donor and acceptor point defects can interact leading to the formation of the defect dipoles as $(Fe_{Ti}^{\prime} \rightarrow V_{O}^{\bullet\bullet})^{\bullet}$, $(Fe_{Ti}^{\prime} \rightarrow La_{Sr}^{\bullet})^{x}$, $(Fe_{Ti}^{\prime} \rightarrow La_{Pb}^{\bullet})^{x}$ or $(V_{Pb}^{\prime\prime} \rightarrow V_{O}^{\bullet\bullet})^{x}$. Therefore, it is imperative to investigate the rule played by defects on nanoscale polarization behavior.

To investigate nanoscale polarization behavior in PST70 and PSLTF1050 thin films, piezoresponse force microscopy (PFM) was used. Whereas X-ray diffraction is only sensitive to long-range periodic structures, the PFM technique is highly sensitive to the local defects that act to promote strong irregularity nanoscale electrical properties [33–36]. Fig. 2(a)-(d) shows simultaneously the surface topography and piezoresponse images. The morphology of the PST70 and PSLTF1050 thin films exhibited a roughness of 8.4 and 6.4 nm, and the grain size is about 90 and 30 nm, as seen in Fig. 2(a)-(b). In addition, both films exhibited dense, cracks free and uniform microstructures. The piezoelectric performance for the PST70 and PSLTF1050 thin films is shown in Fig. 2(c–d). Out-of-plane piezoresponse images of the surface of PST70 thin films revealed highly contrasted PFM images as shown in Fig. 2(c). Here, we find a clear signature of a natural ferroelectric domain structure oriented along different directions (long-range coulombic forces promoting the polar ferroelectric distortion, spontaneous polarization, P_S), i.e., the dark regions represent domains with downward polarization vectors, while the bright regions represent domains with upward polarization vectors. Dark or bright regions of intermediate intensity correspond to other orientations. Hence, this suggests a polycrystalline nature of the film, where the domain structures are randomly oriented. Although PSLTF1050 shows a cubic-like structure, a domains structure was detected by PFM, exhibiting a much lower domain structure contrast when compared to the PST70 thin films (Fig. 2(d)). Substitution of Ti ions

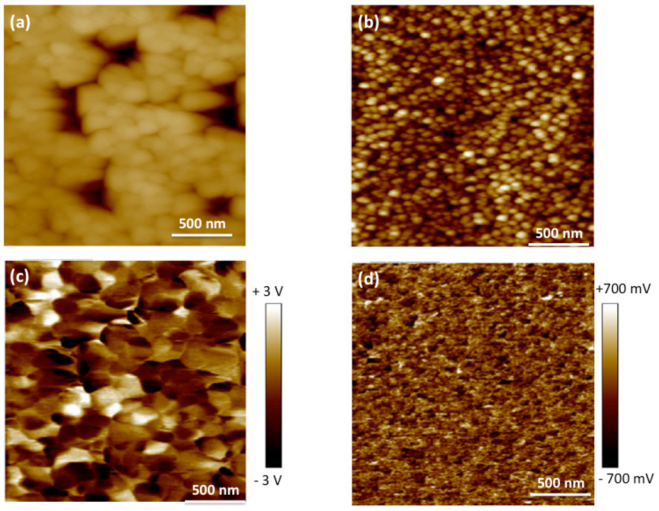

Fig. 2. Surface topography images of (a) PST70 thin films and (b) PSLTF1050 thin films. Out-of-plane PFM images of (c) PST70 thin films and (d) PSLTF1050 thin films.

with Fe ions reduces the off-center displacement of the Ti ions inside the octahedral oxygen cage; this restricts the movement of Ti ions and as a consequence, leads to the suppression of short- and long-range natural electric dipole producing a low piezoresponse image. In addition, the grain size was small to be evidenced in the PFM images. This results are in accordance to previous studies [37,38]. Fe, La co-doping have a significant influence on the microstructure and nanoscopic domain features of PSLTF1050 thin films crystallization processes.

In order to provide deeper insight into the impact of acceptor and donor defect on the polarization switching, the conductive PFM-tip was used to writing patterns of polarization (domain structure) with opposite sign. The PFM results are shown in Fig. 3(a)-(b). Two regions with different contrast can be clearly distinguished in the undoped-PST70 thin films by alternately applying a DC voltage of −15 V (black contrast) and +15 V (bright contrast) to the conductive PFM-tip, corresponding to downward and upward polarization states, respectively (Fig. 3(a)). For undoped-PST70 thin films the highly contrasted domain writing structure pattern is attributed to long-range native electrical dipole coupling as a consequence to its large lattice distortion. These results are consistent with X-ray diffraction (Fig. 1(a)) and Raman spectroscopy (Fig. 1(b)) experimental measurements. On the other hand, considering the pseudocubic-like symmetry for PSLTF1050 thin films (XRD, Fig. 1(a)) a domain switching would not appear; the stability of long-range ferroelectric ordering was broken with co-doping by defect dipoles and point defects, for example. However, these films also showed a domain writing pattern, manifested by reorientation for both positive and negative tip-voltage under the application of ±15 V (a clear switchable behavior). This is depicted in Fig. 3(b). Fig. 3(c) shows the piezohistogram of the thin films obtained from corresponding PFM images after the poled state, represented in Fig. 3(a)-(b). We emphasize that both PST70 and PSLTF1050 films revealed a typical well-developed domains populations ferroelectric curve, corresponding to a relative population of positive (upward) and negative (downward) domains.

Analysis of piezohistograms for undoped-PST70 films reveals the following scenario: i) strong polarization effect indicated by the domain population curves peaks positions; ii) peaks are approximately symmetrical, indicating that most domain population is strong oriented towards positive (upward) and negative (downward) after poling. In contrast to the undoped-PST70 films,

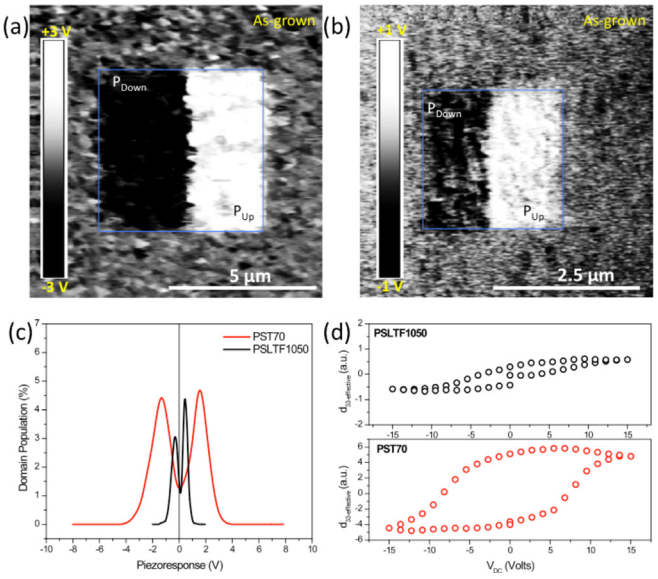

Fig. 3. Out-of-plane PFM images of PST70 (a) and PSLTF1050 (b) thin films written by positive (bright) and negative (dark) bias, ± 15 V. (c) Piezoresponse histogram for PST70 and PSLTF1050 thin films after poling with ±15 V. It consists of two distributions: domains with positive and negative piezoresponse. (d) Local piezoresponse hysteresis loops of the PST70 and PSLTF1050 thin films collected at an individual grain.

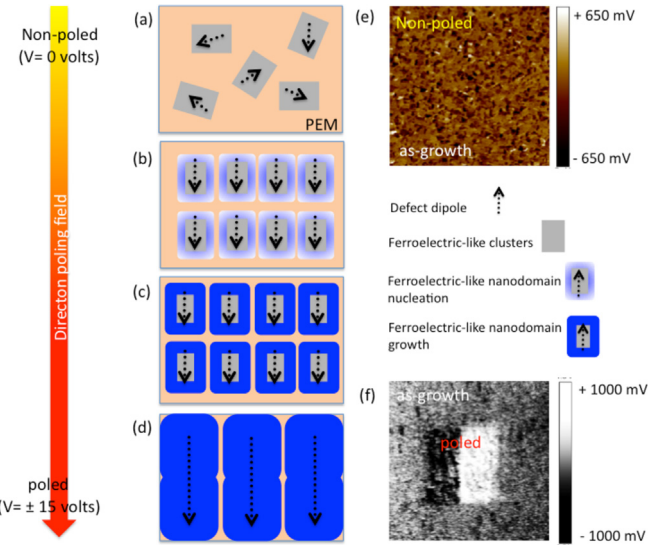

Fig. 4. Schematic illustration of poling and domain structure of PSLTF1050 films. (a) The material initially has a random arrangement of defect dipole giving rise to "ferroelectric-like" clusters inside the paraelectric matrix (PEM). (b) Application of an electric field (poling) aligns defect dipoles with the field. Ferroelectric-like nanodomains nucleation inside the paraelectric matrix (PEM). (c) Once poled, the material has a polar axis. Ferroelectric-like nanodomains growth. (d) After removal of the electric field, the material retains a net polarization producing a poled ferroelectric-like behavior. The material is now piezoelectric and exhibits the downwards and upwards polarization effects (switchable domains).

PSLTF1050 films revealed a different scenario: i) they have smaller piezoresponse observed by the position of the piezo hysteresis curve peaks, indicating weak polarization effect; ii) peaks are asymmetrical, indicating that some domains were not completely oriented during the scan (poling) and there are some non-polar clusters (non-polar state persists throughout the paraelectric phase). Furthermore, Fig. 3(d) shows local piezoelectric hysteresis loop (piezoloops) measured by PFM at one individual point. The well-defined local hysteresis loops clearly confirm the "natural ferroelectric" and "ferroelectric-like" behavior of undoped-PST70 and PSLTF1050 thin films, respectively. They also show polarization reversibility. These results demonstrate that it is possible to switch locally the defect-mediated polarization by applying a DC voltage. During switching these defect dipoles ("ferroelectric-like" defect clusters) align preferentially along the poling direction (up and down) and generate a local piezohysteresis loop. Observation of dipole defect-mediated polarization switching ferroelectricity has been reported by groups other [39–42]. Then, the following scenario for the observed domain writing pattern into cubic matrix (paraelectric phase) can be drawn: the net relative displacement and collective effect of the several charge defects (positive effective charge and negative effective charges, equations (1)–(5)) under external electric field lead to a local dipole moment, giving rise to "ferroelectric-like" defect clusters of small-size. These defects are induced by short-range defect dipoles coupling and in turn, allow an artificial domain structure on the nanometer scale to appear. The schematic diagram of Fig. 4 shows a proposed mechanism which can explain the domain structure in poled regions for cubic paraelectric phase of PSLTF1050 thin films.

Polarization retention behavior was also investigated in these thin films by using the procedure described above (experiment section procedure) to follow the evolution of domain written regions at specific time intervals. Two regions with different contrasts can be clearly distinguished in PST70 and PSLTF1050 thin films by alternately applying a DC voltage of −15 V (black contrast) and +15 V (bright contrast) to the conductive PFM-tip. This approach is illustrated in Fig. 5. The out-of-plane PFM images taken immediately after poling is shown in Fig. 5. As shown in Fig. 5(a), the patterned positive and negative domain structure of PST70 thin films was checked from time to time after the removal of poling voltage. From our observation the contrast remained almost constant during the retention measurement after keeping it for 180 min. In addition, the piezoresponse signal of scanning areas (marked with yellow line) in Fig. 5(a) was measured and the results are shown in Fig. 6(a). The variation of piezoresponse signal with time remained constant implying that the sample reach a stable state after polarization. These results can be interpreted taking into account the absence of nucleation of reversed domain phenomenon, no depolarization field and very low leakage current. Fig. 5(b) shows polarization retention performance of domain structure in PSLTF1050 films. PFM images show changes related to increasing retention time: the contrast of selected area (marked by a yellow line) becomes weaker implying that the nanodomains are in an unstable state after polarization. In Fig. 6(b), is observed a polarization decay as a function of the retention time. Based on these results after the external electric field (conductor PFM-tip probe) be removed, the "ferroelectric-like" defect clusters start to relax to their original unpolarized state.

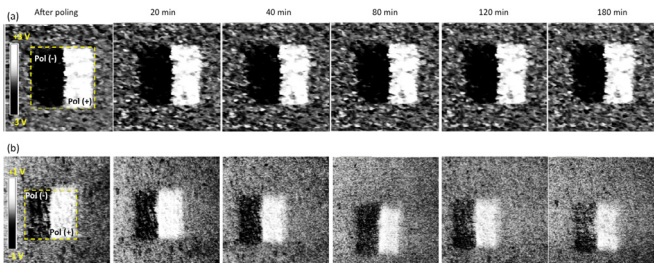

Fig. 5. PFM images of (a) PST70 and (b) PSLTF1050 thin films at different time selected intervals: after poling (0 min), 20 min, 40 min, 80, 120 min and 180 min.

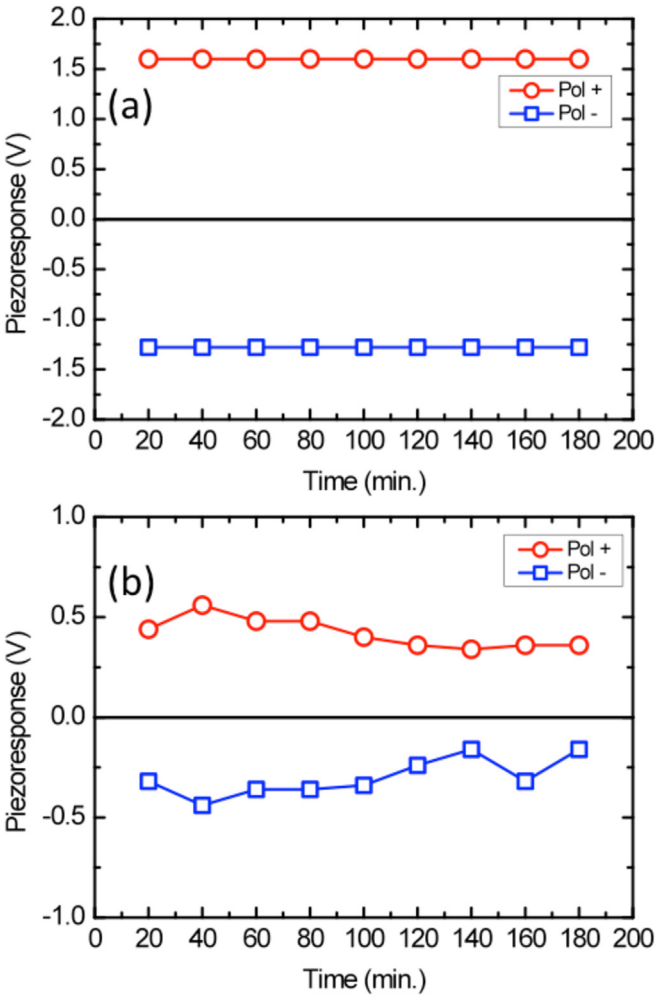

Fig. 6. Positive and negative domain signal as a function time after poling of (a) PST70 and (b) PSLTF1050 thin films.

4. Conclusions

We have experimentally demonstrated by piezoresponse force microscopy technique that the nanoscale polar behavior in Fe, La co-doping PST polycrystalline films are driven by defect dipoles. We have demonstrated that for PSLTF1050 films the presence of defect dipoles allowed the formation of switchable nanodomains (obtained from defect dipoles reorientation). This effect demonstrates the tunning control of the ferroelectric and piezoelectric properties at nanoscale level even inside paraelectric matrix. The tunning feature is guided by the defect dipole (polarization defect). In addition, undoped-PST70 films showed native ferroelectric behavior caused by large tetragonal distortion and collective effect of long-range electric dipole. Finally, the polarization retention behavior (phenomenon also known as back-switching) of films have been investigated as a function time. No obvious domain back-switching has been observed in patterned positive and negative domains after poling for undoped-PST films. However, a decrease of negative and positive domains structure after poling for doped PSLTF1050 films has been observed. These results suggest that it may be possible to fabricate novel materials combining local defect engineering and chemical doping.

Acknowledgments

This study was financially supported by the Brazilian agencies FAPESP and CNPq. In particular, we would like to acknowledge CEPID/CMDMC/INCTMN/CDMF, FAPESP processes no. 11/20536-7, 12/14106-2, 13/07296-2 and 17/10819-8. CNPq process no. 470147/2012-1.

References

[1] H. An, J.Y. Han, B. Kim, J. Song, S.Y. Jeong, C. Franchini, C. Wung, B.S. Lee, Sci. Rep. 6 (2016) 28313–28317.
[2] X. Tang, K. Remmel, X. Lan, J. Deng, H. Xiao, J. Dong, Anal. Chem. 81 (2009) 7844–7848.
[3] A.P. Kulkarni, S. Giddey, S.P. S Badwal, J. Phys. Chem. 120 (2016) 15675–15683.
[4] Md S. Sheikh, D. Ghosh, A. Dutta, S. Bhattacharyya, T.P. Sinha, Mat. Sci. Eng. B 226 (2017) 10–17.
[5] L.V. Costa, R.C. Deus, C.R. Foschini, E. Longo, M. Cilense, A.Z. Simões, Mater. Chem. Phys. 144 (2014) 476–483.
[6] V.R. Palkar, S.K. Malik, Solid State Commun. 134 (2005) 783–786.
[7] C. Sun, J. Wang, H. Kang, J. Chen, M.J. Kimb, X. Xing, Dalton Trans. 39 (2010) 9952–9955.
[8] A. Shuklan, R.N.P. Choudhary, Physica B 405 (2010) 2508–2515.
[9] V.R. Palkar, S.C. Purandare, P. Ayyub, R. Pinto, J. Appl. Phys. 87 (2000) 462–466.
[10] K.H. Reddy, K. Parida, ChemCatChem 5 (2013) 3812–3820.
[11] A.K. Katna, R.K. Kotnala, N.S. Negi, Phys. B Phys. Cond. Matter 425 (2013) 95–99.
[12] S.W. Boland, S.C. Pillai, W.D. Yang, S.M. Haile, J. Mater. Res. 19 (2004) 1492–1498.
[13] I.B. Misirlioglu, S.P. Alpay, Acta Mater. 122 (2017) 266–276.
[14] X. Guo, Yi Chen, G. Wang, D. Rémiens, F. Ponchel, W. Zhang, J. Lian, X. Dong, Mater. Lett. 195 (2017) 182–185.
[15] K. Bala, J. Shah, N.S. Negi, R.K. Kotnala, Integrated Ferroelectrics Int. J. 183 (2017) 110–125.
[16] J.W. Bai, J. Yang, Y.Y. Zhang, W. Bai, Z.F. Lv, K. Tang, J.L. Sun, X.J. Meng, X.D. Tang, J.H. Chu, Ceram. Int. 43 (2017) S516–S519.
[17] N.S. Negi, K. Bala, J. Shah, R.K. Kotnala, J. Electroceram 38 (2017) 51–62.
[18] X. Ren, Nat. Mater. 3 (2004) 91–94.
[19] K. Zhao, H. Yu, J. Zou, H. Zeng, G. Li, X. Li, Materials 10 (2017), 1258–8.
[20] P. Gao, et al., Nat. Commun. 8 (2017), 15549–8.
[21] J.H. Lee, R.H. Shin, W. Jo, Phys. Rev. B 84 (2011), 094112–10.
[22] S.V. Kalinin, et al., Adv. Mater. 22 (2010) 314–322.
[23] A.N. Morozovska, S.V. Svechikov, E.A. Eliseev, B.J. Rodriguez, S. Jesse, S.V. Kalinin, Phys. Rev. B 78 (2008) 054101–054117.
[24] L. Zhang, J. Chen, J. Zhang, H. Wang, L. Xu, X. Xing, Ceram. Int. 42 (2016) 19212–19217.
[25] S.M. Yang, J.G. Yoon, T.W. Noh, Curr. Appl. Phys. 11 (2011) 1111–1125.
[26] K. Klyukin, V. Alexandrov, Phys. Rev. B 95 (2017) 035301–035308.
[27] M. Dutta, Y. Ding, J. Chen, C. Chen, A. Bhalla, R. Guo, Scripta Mater. 130 (2017) 119–123.
[28] D. Lee, et al., Adv. Mater. 24 (2012) 6490–6495.
[29] L. Feigl, T. Sluka, L.J. McGilly, A. Crassous, C.S. Sandu, N. Setter, Sci. Rep. 6 (2016) 1–7.
[30] F.M. Pontes, D.S.L. Pontes, A.J. Chiquito, Marcelo A. Pereira-da-Silva, E. Longo, Mater. Lett. 138 (2015) 179–183.
[31] F.M. Pontes, A.J. Chiquito, W.B. Bastos, Marcelo A. Pereira-da-Silva, E. Longo, J. Mater. Chem. C 4 (2016) 9331–9342.
[32] M. Imada, A. Fujimori, Y. Tokura, Rev. Mod. Phys. 70 (1998) 1039–1263.
[33] Y.F. Hou, T.D. Zhang, W.L. Li, W.P. Cao, Y. Yu, D. Xu, W. Wang, X.L. Liu, W.D. Fei, RSC Adv. 5 (2015) 61821–61827.
[34] Q. Li, Y. Liu, J. Schiemer, P. Smith, Z. Li, R.L. Withers, Z. Xu, Appl. Phys. Lett. 98 (2011), 092908–3.
[35] K. Zhan, M. Su, B. Zhao, H. Han, Q. Yuan, X.Y. Wang, Ferroelectrics 500 (2016) 276–282.
[36] P.R. Choudhury, J. Parui, S. Chiniwar, S.B. Krupanidhi, Solid State Commun. 208 (2015) 15–20.
[37] W. Sun, J.F. Li, Q. Yu, L.Q. Cheng, J. Mater. Chem. C 3 (2015) 2115–2122.
[38] Q. Yu, J.F. Li, F.Y. Zhu, J. Li, J. Mater. Chem. C 2 (2014) 5836–5841.
[39] D. Maurya, Y. Zhou, B. Chen, M.G. Kang, P. Nguyen, M.K. Hudait, S. Priya, Appl. Mater. Interfaces 7 (2015) 22458–22468.
[40] P. Erhart, P. Traskelin, K. Albe, Phys. Rev. B 88 (2003) 024107–024110.
[41] X.F. Zhao, A.K. Soh, L. Li, J.X. Liu, Phil. Mag. Lett. 90 (2010) 251–260.
[42] A. Grunebohm, T. Nishimatsu, Phys. Rev. B 93 (2016) 134101–134112.